Buckling of long thin plates under residual stresses with application to strip rolling

Kékéli Kpogan, Michel Potier-Ferry

Buckling of long thin plates under residual stresses with application to strip rolling

K. Kpogan[1, a *] and M. Potier-Ferry[1,b]

[1] Université de Lorraine, Laboratoire d'Etude des Microstructures et de Mécanique des Matériaux(LEM3), UMR CNRS 7239, Ile du Saulcy 57045 Metz, France

[a]kekeli.kpogan@univ-lorraine.fr, [b]michel.potier-ferry@univ-lorraine.fr

* corresponding author

Keywords: rolling, flatness defects, residual stresses, post-buckling

Abstract. We present a simplified numerical method which can be used to predict efficiently the response of long thin plates under effects of residual stresses induced by production process such as rolling or continuous annealing. The principle consists in assuming harmonic buckling mode along the sheet length, and we consider Koiter-Budiansky post-buckling theory to compute the stress-deflection curve. In this way, only the width of the sheet has to be discretized by 1D finite elements. The size and shape of the flatness defects can be predicted efficiently and for a large number of cases. Various types of residual stresses and loadings can be accounted for. In particular, we will see the influence of the global traction on the buckling and post-buckling behavior. The numerical results are compared with experimental data and full numerical computations

Introduction

Metal sheet is generally produced by a rolling process. The final product is a thin plate. The strip, usually, may show wavy configuration with typical wave patterns. The most important ones are edge-waves and center-waves respectively. These waves are the result of buckling due to self-equilibrating longitudinal residual stresses with a compressive longitudinal membrane force state in the middle of the strip ("center-waves") or in the edge zones ("edge-waves"), respectively. During the production process, the buckling waves are usually suppressed by global traction. However, they may appear when the global traction is no longer present. The deformation of the roll mill (flatness, bending ...) induces a non-uniform out-of-bite elongation in the width of the strip. The residual stresses are generated by this non-uniform elongation leading to buckling of the strip.

In a number of recent works Fisher et al. [3,4,6] presented a method combining finite element simulation and semi-analytical Rayleigh-Ritz technique. In this approach the authors performed comprehensive investigation of residual stress buckling within the context of metal forming, and pointed out a number of interesting features regarding the localisation of the instability patterns. They give a polynomial form in transverse direction of the plate; meanwhile, all the geometric parameters are determined by minimizing the elastic energy of the deformation path from flat to wavy shape. It is shown that the shape of the residual stress distribution over the strip width influences the buckling mode. Furthermore, they demonstrated that increasing global traction does not only lead to increased critical residual stress intensity, but also produces shorter buckling waves concentrated towards the edge of the strip. A more detailed analysis, which will be presented in this work, confirms these results.

In several others papers, different buckling phenomena appearing during the rolling process have been investigated. For instance, by Abdelkhalek et al. [1], who focused on shell elements and predicted buckling behaviours of plates under residual stresses. The model is based on Asymptotic Numerical Method. This model will be used to validate the model that we propose in the present work.

In this paper, we present a simplified numerical method called "SNM" which can predict the response of long thin plates under residual stresses.

Definitions and analysis

We consider a thin strip (Fig. 2) of width *B*, thickness *h* and length *L*. The elastic constants of the material are E (the Young's modulus) and ν (the Poisson's ratio). The plate bending stiffness is $D = Eh^3 / \left(12\left(1-\nu^2\right)\right)$. The strip is loaded by a self-equilibrating residual stresses λN_x^{res} and a constant global traction. Following Fisher et al. [3], the former contribution is independent of the axial coordinate *x*, but depends on *y* and is assumed to be under the form $\lambda N_x^{res}(y)$; λ is the main control parameter in what follows, in the sense that buckling will be triggered once its value exceeds a certain critical threshold. We note this critical threshold value λ_c. The field of study is $\Omega = \left\{(x,y) \in \Omega_x \times \Omega_y \mid \Omega_x = \left[-\frac{L}{2},\frac{L}{2}\right]; \Omega_y = \left[-\frac{B}{2},\frac{B}{2}\right]\right\}$.

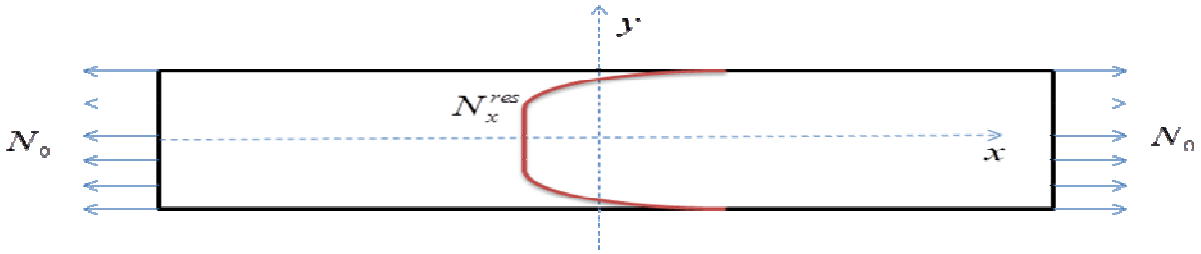

Fig. 1 The geometry of the strip and the membrane force distribution $\lambda N_x^{res}(y) + N_0$

The condition that the residual stresses must be self-equilibrated is as follows:

$$\int_{\Omega_y} N_x^{res}(y)dy = 0 \tag{1}$$

Following Rammerstorfer et al., 2000, the out-of-plane displacement is approximated as:

$$w(x,y) = f(y)cos(qx) \tag{2}$$

where q represents the half-wave length of the buckling pattern. It is also an additional unknown of the problem that we must thereafter minimize to find the critical buckling load. The principle is to assume that the buckling mode is harmonic along the length of the strip. Unlike to what was done by Fisher et al [4], where the shape of $f(y)$ is given by a polynomial function, in our approach the width of the sheet has to be discretized by 1D Hermite finite elements. These elements provide inter-element continuity of the field variable (displacement) and its first derivatives (stress, and so on) at the nodal points. The reasons why we have introduced these elements are that we used higher-order differential equations. For example, in post-buckling or in asymptotic considerations, the determination of the amplitude of the buckling mode is governed by a fourth-order differential equation. Thus, inter-element continuity of the first derivative is required.

Rolling buckling formulation

We introduce functional ϕ as the total potential energy for a rectangular thin plate in elastic stability. Meanwhile, we assume negligible N_y and N_{xy} which are, respectively, in-plane compressive forces in y-directions and in-plane shear forces.

$$\phi = \phi_B + \phi_M$$

with

$$\phi_B = \frac{D}{2}\int_\Omega \left\{\left(\frac{\partial^2 w}{\partial x^2}+\frac{\partial^2 w}{\partial y^2}\right)^2 - 2(1-\nu)\left[\frac{\partial^2 w}{\partial x^2}\frac{\partial^2 w}{\partial y^2} - \left(\frac{\partial^2 w}{\partial x \partial y}\right)^2\right]\right\} d\Omega \tag{3}$$

$$\phi_M = \frac{1}{2}\int_\Omega (N_x^{res} + N_0)\left(\frac{\partial w}{\partial x}\right)^2 d\Omega$$

ϕ_B, ϕ_M are, respectively, the bending energy, and the membrane energy due to traction N_0 and the residual stress.
The stationarity of ϕ allows writing the equilibrium conditions of the plate:

$$\delta\phi = \delta\phi_B + \delta\phi_M = 0 \tag{4}$$

where:

$$\delta\phi_B = D\int_\Omega \left(\frac{\partial^2 w}{\partial x^2}+\frac{\partial^2 w}{\partial y^2}\right)\left(\frac{\partial^2 \delta w}{\partial x^2}+\frac{\partial^2 \delta w}{\partial y^2}\right)dxdy$$
$$-D(1-\nu)\int_\Omega \left\{\frac{\partial^2 w}{\partial x^2}\frac{\partial^2 \delta w}{\partial y^2}+\frac{\partial^2 w}{\partial x^2}\frac{\partial^2 \delta w}{\partial y^2}-2\frac{\partial^2 w}{\partial x\partial y}\frac{\partial^2 \delta w}{\partial x\partial y}\right\}dxdy$$
$$\delta\phi_M = \int_\Omega \left(\lambda N_x^{res}+N_0\right)\frac{\partial w}{\partial x}\frac{\partial \delta w}{\partial x}dxdy$$
$$\delta w(x,y) = \delta f(y)cos(qx)$$

Using Eq. 2, which allows taking the buckling mode harmonic along the plate, $\delta\phi$ is rewritten as follows:

$$\frac{D}{q^2}\int_{\Omega_y}\frac{\partial^2 f}{\partial y^2}\frac{\partial^2 \delta f}{\partial y^2}dy - D\nu\int_{\Omega_y}\left\{f\frac{\partial^2 \delta f}{\partial y^2}+\frac{\partial^2 f}{\partial y^2}f\delta\right\}dy +$$
$$+2D(1-\nu)\int_{\Omega_y}\frac{\partial f}{\partial y}\frac{\partial \delta f}{\partial y}dy + (Dq^2+N_0)\int_{\Omega_y} f\delta f dy + \int_{\Omega_y}\lambda N_x^{res} f\delta f dy = 0 \tag{5}$$

The unknowns of this system are q, f and λ. We minimize q, which is supposed to be provided and discretized f using 1D Hermite finite elements. λ will be determined as eigenvalues, and $\lambda_c N_x^{res}(y)+N_0$ corresponding to the minimum eigenvalue is the critical buckling load.

Estimation of the amplitude of the post-buckling pattern

In this section we propose to estimate the size of the defect. We recover the mode $f(y)$ and the critical load λ_c obtained in the linear buckling. We use the equations of Von Kàrmàn which are nonlinear equations describing the large deflections of thin plates. The strain components derived from standard kinematics as:

$$\gamma = \begin{pmatrix} \frac{\partial u}{\partial x}+\frac{1}{2}\left(\frac{\partial w}{\partial x}\right)^2 & \frac{1}{2}\left(\frac{\partial u}{\partial x}+\frac{\partial v}{\partial x}+\frac{\partial w}{\partial x}\frac{\partial w}{\partial y}\right) \\ \frac{1}{2}\left(\frac{\partial u}{\partial x}+\frac{\partial v}{\partial x}+\frac{\partial w}{\partial x}\frac{\partial w}{\partial y}\right) & \frac{\partial v}{\partial y}+\frac{1}{2}\left(\frac{\partial w}{\partial y}\right)^2 \end{pmatrix} \tag{6}$$

$u(x,y)$ and $v(x,y)$ are, respectively, the displacement in the *x*-direction and *y*-direction. We assume that the residual stresses result from plastic deformation. Thus, we write the law of elastic behavior of the plate with a residual term γ^{res}.

$$\begin{cases}\gamma = \gamma_{el}+\gamma^{res} \\ S = S_{el}+S^{res}\end{cases} \tag{7}$$

S and γ are respectively the second stress tensor of Piola-Kirchoff and the strain tensor of Green-Lagrange. S^{res} and γ^{res} are respectively the residual stress and the residual strain. S_{el} and γ_{el} are respectively the elastic components of S and γ. To determine the stress field, we introduce the concept of stress functions that verifies the compatibility equations of the plate. We assume that F is the Airy stress function. Thus based on Eq. 6 and Eq. 7, we can write the equations of Von Karman:

$$\frac{1}{Eh}\int_{\Omega}\Delta F\Delta\delta F d\Omega=\frac{1}{2}\int_{\Omega}[w,w]\delta F\ d\Omega + \lambda\int_{\Omega}\left\{\gamma_x^{res}\frac{\partial^2\delta F}{\partial y^2}+\gamma_y^{res}\frac{\partial^2\delta F}{\partial x^2}-2\gamma_x^{res}\frac{\partial^2\delta F}{\partial x\partial y}\right\}d\Omega \tag{8}$$

$$D\int_{\Omega}\left\{\Delta w\Delta\delta w-2(1-\nu)[w,\delta w]\right\}d\Omega-\int_{\Omega}[F,w]\delta w d\Omega=0 \tag{9}$$

with $\left[u(x,y),v(x,y)\right]=\frac{\partial^2 u}{\partial x^2}\frac{\partial^2 v}{\partial y^2}+\frac{\partial^2 u}{\partial y^2}\frac{\partial^2 v}{\partial x^2}-2\frac{\partial^2 u}{\partial x\partial y}\frac{\partial^2 v}{\partial x\partial y}$

Eq. 8 and Eq. 9 are respectively the equilibrium equation of Von Kàrmàn in weak-form integration and energy formulation. The first equation allows us to determine the Airy stress function F. And finally once F calculated, starting from Eq. 9, we calculate the amplitude of the defect.

The post-buckling theory shows that from a critical point, the bifurcated branch can be represented as a power series in terms of a path parameter a which is the amplitude of the buckling pattern. Eq. 8 and Eq. 9 are nonlinear; to solve them we introduce an asymptotic series expansion of the unknowns of the problem. Thus, we consider the Koiter-Budiansky post-buckling theory. The method consists to assume that $w=aw_1$ which w_1 is the transverse deflection obtained in the linear buckling. Finally, from $w=aw_1$, we can express the other unknowns of the problem in the form of series expansion relative to a.

$$\begin{Bmatrix}F\\ \lambda\\ N\end{Bmatrix}=\begin{Bmatrix}F_0\\ \lambda_0\\ N_0\end{Bmatrix}+a^2\begin{Bmatrix}F_2\\ \lambda_2\\ N_2\end{Bmatrix} \tag{10}$$

In the following, we consider that $\gamma_x^{res}=-\frac{1}{Eh}N_x^{res};\ \ \gamma_y^{res}=-\nu\gamma_x^{res};\ \ \ \gamma_{xy}^{res}=0$.

They are respectively, the residual strain in the x-direction, in the y-direction and the residual shear strain. We introduce two additional parameters A_0 and A_2 that allow us to determine the Airy stress function F, so F_2. Thus using Eq. 8 we get:

$$F_2(x,y)=A_0(y)+A_2(y)cos(2qx)+\lambda_2F_0(y) \tag{11}$$

We discretize A_0 and A_2 by 1D finite elements Hermite. Once Eq. 8 discretized by 1D finite elements is solved, λ_2 is calculated using Eq. 9 that allow us to make the post-buckling analysis and to determine the nature of the bifurcation. Finally, for a given load λ, we can determine the size of the defect.

Numerical examples

Let us consider a plate made of material whose elastic constants are the Young's modulus E = 210GPa, and Poisson's ratio ν = 0.3. It has thickness h=0.252mm and subjected to a residual

stresses N_x^{res} . To validate the model our results are compared first to analytical results (Timoshenko et al. [7]) and secondly to the shell model. The shell model is a finite element model based on the asymptotic numerical method and a shell formulation (Zahrouni et al. [9]). This model is able to simulate buckling and post-buckling of shells under residual stresses. It is a complete model using the Hu-Washizu formulation. Two types of loadings are used in the model: the global traction and the residual stresses.

The strip buckled under homogeneous residual stresses

The tests were conducted to validate the simplified model. We took a very simple case in which analytical solutions (Timoshenko et al. [7]). The sheet boundary conditions are given in Fig. 2.

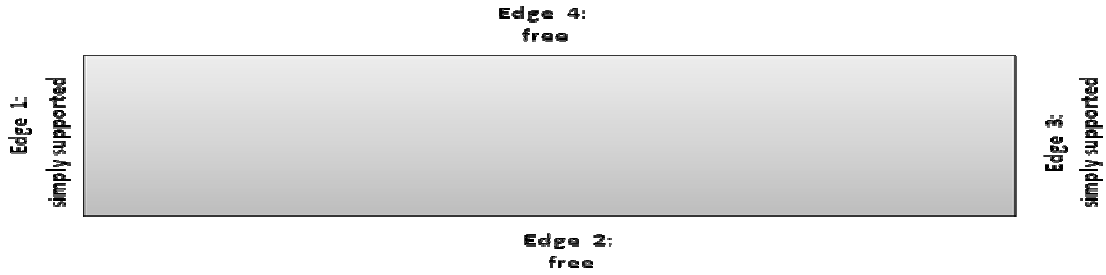

Fig. 2 Boundary conditions used for the validation tests

So the strip is considered free on the edge 2 & 4 and simply supported on the edge 1 & 3 and subjected to a residual stresses for which only the longitudinal component is not zero:

$$\sigma^{res}\left[MPa\right] = hN_x^{res} = -\left(\frac{\pi}{B}\right)^2\left(\frac{L}{B}+\frac{B}{L}\right) \tag{12}$$

We vary the aspect ratio $k=L/B$ while assuming that the width of the sheet is constant. So we vary the length of the sheet to compare the evolution of the critical buckling load. Figure 3 shows a very good agreement between the shell model and our model. For B = 100mm we obtain the following results:

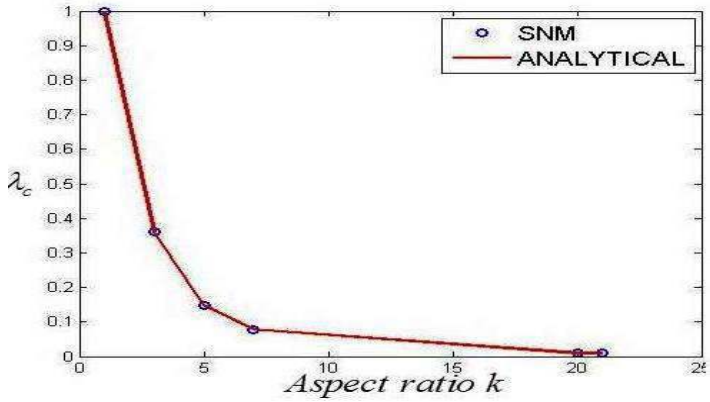

Fig. 3 Dependence of λ_c on k

We note that the final critical load $\lambda_c N_x^{res}$ is always equal to -72.30MPa when the aspect ratio k increases. This is explained by the fact that the critical load decreases with respect to the aspect ratio k (see Fig. 3). The analytical model and the shell model also gives exactly the same values found that our model.

The strip buckled under heterogeneous residual stresses

We perform in these part test cases with heterogeneous residual stresses. These residual stresses will be assumed uniform in the x-direction (the rolling direction) and heterogeneous in the y-

direction. Following the work of Bush et al. [2], we consider these residual stresses self-equilibrated, with an analytical form in width:

$$N_x^{res}(y) = \alpha\left(-\beta\left(\frac{2y}{B}-1\right)^r + 1\right) \tag{13}$$

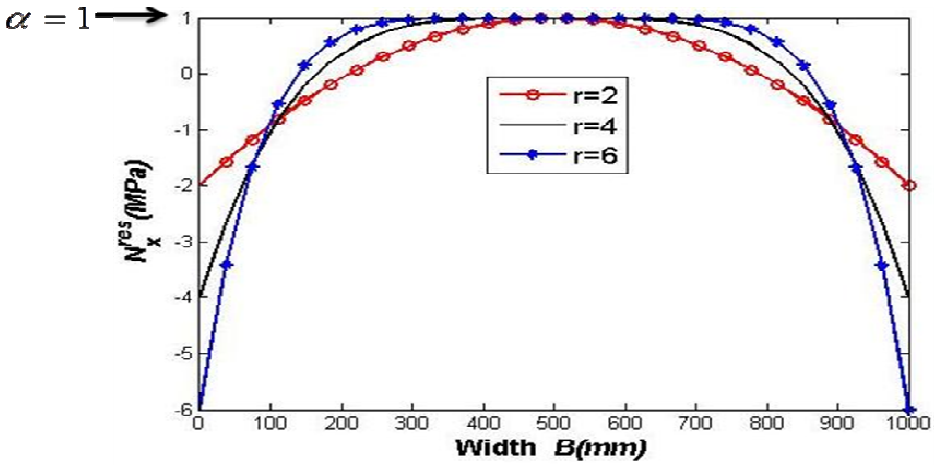

Fig. 4 Residual stresses profile: Effect of r on N_x^{res}

Figure 4 shows the profile shape of the residual stresses that we used in this section. In order to obtain self-equilibrium of N_x^{res}, it is necessary that $\beta = r+1$, with r an even number. r is used to locate defects along the strip. α can be incorporated as an imposed value of the residual stresses. As said previously for edge-waves defects, it is necessary to have a profile presenting a compressive longitudinal force in the edge zones in the strip and conversely in the middle, the center-waves defects. Besides these two types of defect, our method can deal with several other types of defect. But in these test cases, we focus on just these two types of defects.

Influence of the global traction

In order to simulate the rolling process, global traction should be taken into account. The work of Fischer et al. [3] showed that increasing global tensile force does not only lead to increased critical residual stress intensity, but also produces shorter buckling waves concentrated towards the edge of the strip. In the work of Bush et al. they do not take into account this global traction. But we note that the residual stress profiles used are not self-equilibrated. So they are explicitly introduced in the stress profiles. In our case, we consider the residual stresses self-equilibrated and we distinguish these from the global traction.

In the following, by considering Eq. 13, we take, $r = 4$, $\alpha = 30$ for edge-waves defects and $\alpha = -60$ for middle-waves defects. Meanwhile, we take the thickness h = 0.5, width B=1000mm, and length L=5000mm.

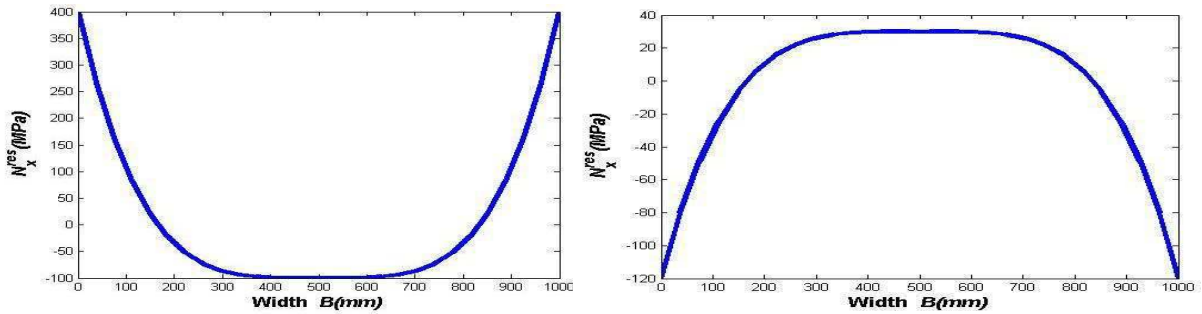

Fig. 5 Residual stresses profiles of Bush; 1) For center-waves defects; 2) For edge-waves defect

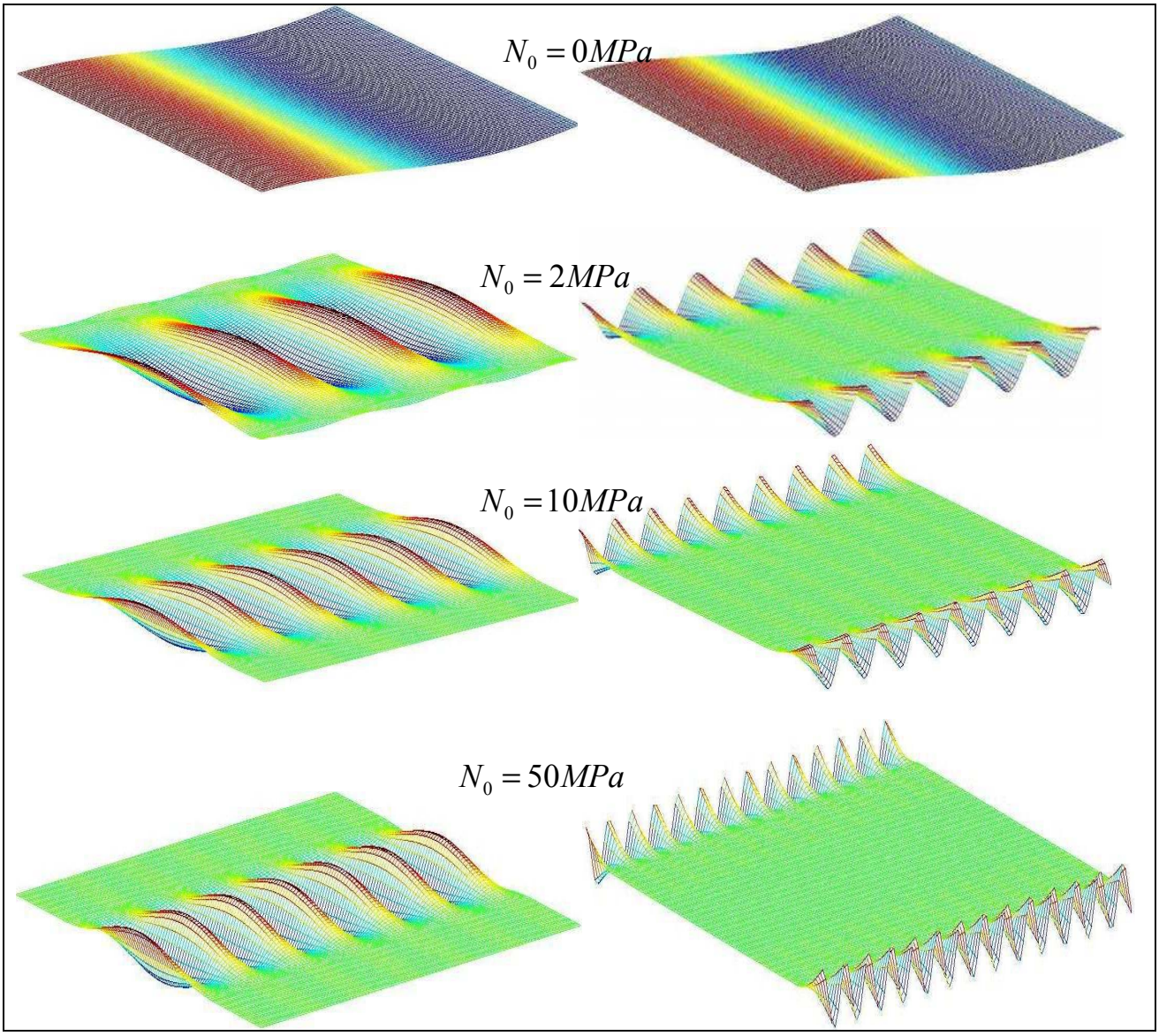

Fig.6. Influence of global traction on the buckling mode

Fig. 7 shows the dependence of the critical load on the global tensile. The obtained results are in good agreement with the shell model. The relative error is 10^{-3}. The results show that from a certain value of the global traction, the minimal critical load is linear with respect to the traction. This is also observed on the buckling modes. Note that these modes become identical progressively from a certain value of the global traction N_0. Furthermore, we can see in Fig. 6 that the period of buckling increases with the traction. Table 1 confirms these observations. This table shows that the wavelength l decreases with respect to the global traction. Thus, the global traction stabilizes the defects observed during the rolling process.

Table 2 Dependence of λ_c and the wavelength l on the global traction

Global traction	$N_0[Mpa]$	10	20	50	80
Case of center-waves defects	λ_c	0.11	0.21	0.51	0.81
	amplitude $a[mm]$	11.4	9.51	6.01	3.25
	wavelength $l[mm]$	981.74	872.66	785.4	714
Case of edge-waves defects	λ_c	0.14	0.25	0.56	0.86
	amplitude $a[mm]$	12.04	10.63	5.99	2.80
	wavelength $l[mm]$	981.74	872.66	785.4	714

The global traction plays a key role in rolling process. As Fig. 6 shows, when it is zero, we always get a global mode. As Bush et al. [2] does not use N_0 explicitly in the problem, they obtained defects by imposing additional boundary conditions. For example, to obtain edge-waves defects, they fixed the center of the strip, and to obtain center-waves defects, they fixed the edge of the strip. In our case, we don't need these additional conditions to obtain the expected defects buckling.

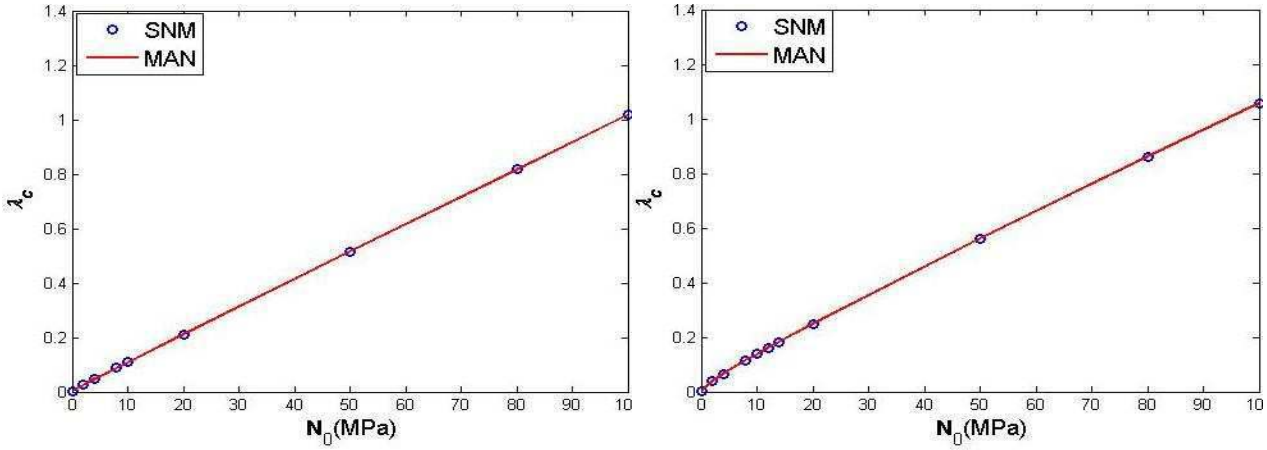

Fig.7 Dependence of the critical load λ_c on N_0 ; 1) for center-waves defects; 2) for edge-waves defects; the results are compared with the shell model MAN

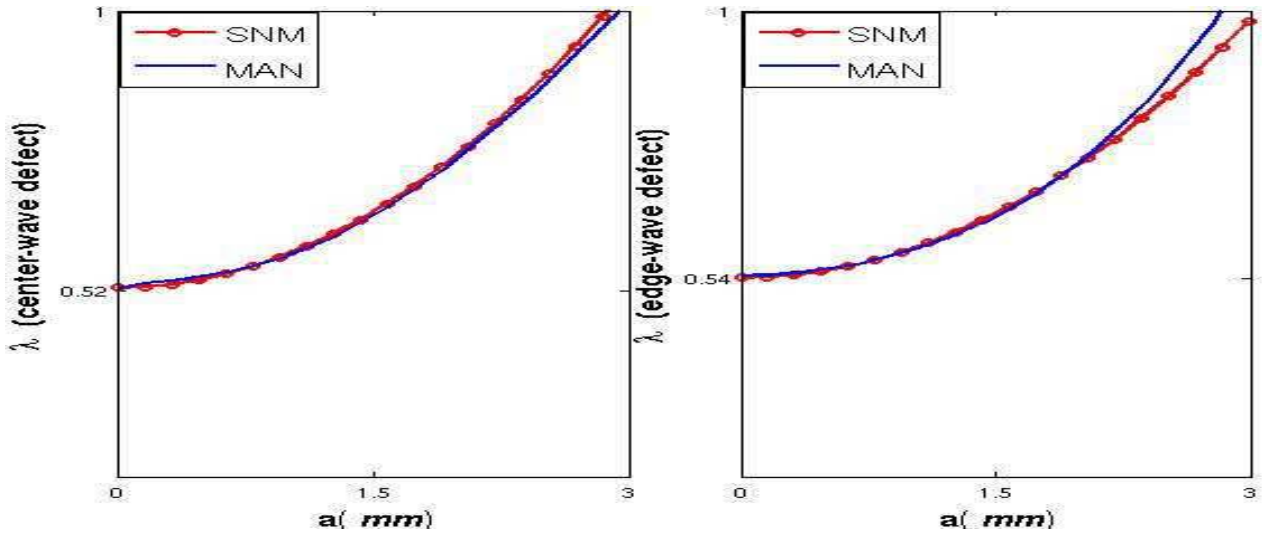

Fig.8. Dependence of the load parameter ($\lambda = \lambda_0 + a^2\lambda_2$) on the amplitude a of the buckling mode; 1) for center-waves defects; 2) for edge-waves defect; the global traction $N_0 = 50MPa$; the results are compared with the shell model MAN

Figure 8 shows the dependence of the load parameter on the size of the defect. We note that $\lambda_c \le \lambda \le 1$. If $\lambda \le \lambda_c$ and $\lambda \ge 1$ the amplitude of the buckling mode is equal to zero. The details show that even with the "full model of buckling" is the shell model, we can well describe and predict the post buckling to a certain level of loading. Even beyond this level of loading, the relative difference of the buckle amplitude mode with the shell model is insignificant.

Furthermore, according to what Fischer et al. [3] have found, we note that when the global tensile increases the amplitude of the buckling mode also increases (see Table 2). Thus the global tensile greatly influences the size of the defect.

Influence of the geometry of the strip

Examples tested with the shell model show that the buckling mode does not depend on the length of the sheet. The goal is to simulate the entire length of the rolled sheet. But it needs very expensive

calculations in time resolution. It will therefore be useful to find a suitable length for our calculations. This problem does not arise in our case because we have already made an assumption on the mode shape in the *x*-direction of the sheet. It remains only to study the influence of the width on the buckling of the sheet.

We consider a plate having the same elastic property as in previous cases. We fix here the global traction $N_0 = 50MPa$ and we consider the same profiles of residual stresses as in previous cases.

Table 2 Influence of the width of the strip on the rolling buckling and the post-buckling

	$B[mm]$	250	500	1000	2000	2500	3000	3500	4000
Case of edge-waves defects	λ_c	0.86	0.67	0.56	0.50	0.49	0.48	0.47	0.47
	$a[mm]$	1.71	3.71	5.98	7.81	8.99	9.70	10.26	11
	$l[mm]$	224.4	290.88	374	462	523.6	561	561	604.15
Case of center-waves defects	λ_c	0.60	0.54	0.51	0.51	0.50	0.50	0.50	0.50
	$a[mm]$	2.58	3.92	6.00	8.78	10.02	11	11.83	13.02
	$l[mm]$	327.2	490.87	785.4	1309	1570	1570	1963	1963.5

Table 2 shows that the plate width also has influences on the rolling process. We note that the strip buckles more easily with a larger width. This resulting in decrease of the critical buckling load with the width. This also causes increase of the defect amplitude and the buckling mode wavelength. It shows that the critical load remains almost constant when the width of the sheet reaches a certain value. Thus, the width of the sheet plays an important role in buckling, as much as width of the roll mill.

Conclusion

We modeled the buckling phenomenon under residual stresses that often occur during rolling. First, we started with a linear analysis which consist to determinate the critical load parameter as a minimum eigenvalue. We based on the conditions of equilibrium of the plate and assuming that the buckling mode is harmonic along the length of the sheet. In order to compare our results with analytical solution, we imposed additional boundary conditions in the sheet. Our results are in good agreement with the analytical solution. We have also determinate the estimation of the amplitude of the buckling. The procedure is based on the equations of Von Karman and Koiter-Budiansky theory. To validate the model, we used the cases tests that may have edge-waves and center-waves defects on the sheet. The results obtained indicate that the global traction and the geometry of the plate greatly influence the rolling buckling. We showed that the global traction increases and the amplitude of the buckling mode decreases with the critical buckling load. In both tests based on different residual stresses profiles, the results show that the wavelength decreases also with the global traction.

References

[1] S. Abdelkhalek, P. Montmitonnet, N. Legrand, P. Buessler, Coupled approach for flatness prediction in cold rolling of thin strip, Int. J. Mech. Sci. 53 (2011) 661-675.

[2] A. Bush, R. Nicholls, J. Tunstall, Stress levels for elastic buckling of rolled strip and plate, Ironm. Steelm. 28 (2001) 481-484.

[3] F. Fischer, F. Rammerstorfer, N. Friedl, Residual stress-induced centre wave buckling of rolled strip metal, Appl. Mech. 70 (2003) 84-90.

[4] F. Fischer, F. Rammerstorfer, N. Friedl, W. Wieser, Buckling phenomena related to rolling and levelling of sheet metal, Int. J. Mech. Sci. 42 (2000) 1887–1910.

[5] J. W. Hutchinson, W. T. Koiter, Post-buckling theory. App. Mech. Rev. 23 (1970) 1353-1362.

[6] F. Fischer, F. Rammerstorfer, N. Friedl, Buckling of Free Infinite Strips Under Residual Stresses and Global Tension. Appl. Mech. 68 (2001) 399-404.

[7] S. P. Timoshenko, J. M. Gere, Theory of elastic stability, 2nd Edition, Mc Graw Hill Book Company, Inc,New York, 1961.

[8] S. Yuan, Y. Jin, Computation of elastic buckling loads of rectangular thin plates using the extended Kantorovich method, Comput. Struct. 66 (1998) 861-867.

[9] H. Zahrouni, B. Cochelin, M. Potier-Ferry, Computing finite rotations of shells by an asymptotic-numerical method, Computer Methods in Applied Mechanics and Engineering. 175 (1999) 71-85.